2010

Permittivity and permeability of Fe(Tb) nanoparticles and their microwave absorption in the 2–18 GHz range

Z. Han
Shenyang National Laboratory for Materials Science, Institute of Metal Research and International Center for Materials Physics, Chinese Academy of Sciences, Shenyang 110016, People's Republic of China

D. Li
Shenyang National Laboratory for Materials Science, Institute of Metal Research and International Center for Materials Physics, Chinese Academy of Sciences, Shenyang 110016, People's Republic of China

M. Tong
Shenyang National Laboratory for Materials Science, Institute of Metal Research and International Center for Materials Physics, Chinese Academy of Sciences, Shenyang 110016, People's Republic of China

X. Wei
Shenyang National Laboratory for Materials Science, Institute of Metal Research and International Center for Materials Physics, Chinese Academy of Sciences, Shenyang 110016, People's Republic of China

Ralph Skomski
University of Nebraska at Lincoln, rskomski2@unl.edu

See next page for additional authors

Permittivity and permeability of Fe(Tb) nanoparticles and their microwave absorption in the 2–18 GHz range

Z. Han,[1] D. Li,[1] M. Tong,[1] X. Wei,[2] R. Skomski,[2] W. Liu,[1,2,a)] Z. D. Zhang,[1] and D. J. Sellmyer[2]

[1]*Shenyang National Laboratory for Materials Science, Institute of Metal Research and International Center for Materials Physics, Chinese Academy of Sciences, Shenyang 110016, People's Republic of China*

[2]*Department of Physics and Astronomy and Nebraska Center for Materials and Nanoscience, University of Nebraska-Lincoln, Lincoln, Nebraska 68588-0113, USA*

(Presented 19 January 2010; received 30 October 2009; accepted 23 December 2009; published online 21 April 2010)

The permittivity and permeability of the Tb-doped and undoped Fe core-shell nanoparticles were investigated for frequencies from 2 to 18 GHz. The particles were synthesized by arc discharge and contain some oxygen, probably in the form of Fe_2O_3, Fe_3O_4, and Tb_2O_3, whereas the core material is Fe. Both the electromagnetic materials constants and the morphology of the Fe nanoparticles are changed by Tb addition, which gives rise to the shifts to higher frequencies and thinner thicknesses of the maximum microwave absorption in the Tb-doped Fe nanoparticles. © *2010 American Institute of Physics*. [doi:10.1063/1.3369972]

I. INTRODUCTION

Nanoscale composites of transition metals and dielectric materials, especially core-shell structures, tend to exhibit good electromagnetic (EM)-wave absorption properties because they have higher absorption frequencies, broader absorption bands, and thinner layer thicknesses than the classical bulk ferrite absorbants.[1–7] Among these nanocomposites, Fe-based nanocapsules are of great interest due to their typical ferromagnetic characteristics and potential applications in microwave absorption.[2–4] It is well known that the reflection loss (RL) can be used to characterize the absorption properties of EM materials. According to the transmission-line model,[8] the RL of a metal-backed microwave absorbing layer is

$$\mathrm{RL} = 20\log_{10}\left(\frac{jZ\tanh(kd)-1}{jZ\tanh(kd)+1}\right) \quad \text{with} \quad Z = \sqrt{\frac{\mu_r}{\varepsilon_r}} \quad \text{and} \quad k = \frac{2\pi f}{c}\sqrt{\mu_r\varepsilon_r}. \tag{1}$$

Here, the materials constants $\mu_r=\mu'-j\mu''$ and $\varepsilon_r=\varepsilon'-j\varepsilon''$ are the complex permeability and complex permittivity, respectively, d is the absorption layer thickness, and f is the frequency of incident wave. It is of great interest to study the influence of varying the parameters of Eq. (1) on the EM-wave absorption properties. Nanoparticles prepared from pure iron or nickel possess a core-shell structure due to natural oxidation of the nanoparticle surfaces, and the complex permittivity and complex permeability spectra show that the absorption performance in iron nanoparticles is better than that of nickel nanoparticles.[4] However, the synthesis, morphology, and materials constants in the nanoparticles of rare earth and iron have seldom been reported. In the present work, the permittivity and permeability and microwave absorption of Tb-doped and undoped Fe-nanoparticles are investigated in the frequency range of 2–18 GHz.

II. EXPERIMENT

Both the Tb-doped and undoped Fe nanoparticles were prepared by arc discharging a $Fe_{90}Tb_{10}$ and a 99.99% purity Fe ingot in carbon crucible, as described in Ref. 3. The core-shell nanoparticles were investigated by a transmission electron microscope (TEM) (TECNAI F30) with an emission voltage of 300 kV. The surface compositions of the nanoparticles were determined by x-ray photoelectron spectroscopy (XPS), with an Al $K\alpha$ line x-ray source. Magnetic hysteresis at 295 K of the nanoparticles was measured in magnetic fields between 10 and −10 kOe, using a superconducting quantum interference device (Quantum Design MPMS-7). Coaxial method was used to determine the EM parameters of the toroidal samples (see details for the preparation of the toroidal samples in Ref. 3) in a frequency range of 2–18 GHz using an Agilent 8722ES vector network analyzer (VNA) with a transverse EM mode. The complex permittivity and complex permeability were calculated from the S-parameters tested by the calibrated VNA, using a simulation program for the Reflection/Transmission Nicolson–Ross model.[9]

III. RESULTS AND DISCUSSION

The Tb-doped nanoparticles in Figs. 1(a) and 1(b) are spherical nanocapsules with diameters of 10–50 nm and shells of about 2–3 nm, whereas the Tb-free nanoparticles, Figs. 1(c) and 1(d), have a similar shape but larger diameters (40–80 nm). The introduction of Tb seemed to confine the size of the nanocrystal cores of the nanocapsules. Magnetic hysteresis loops in Fig. 2(a) show that the saturation magnetization (M_S) for the Tb-doped Fe nanocapsules is 136 A m^2/kg, while that of the undoped Fe nanoparticles is about 200 A m^2/kg.

a)Electronic mail: wliu@imr.ac.cn.

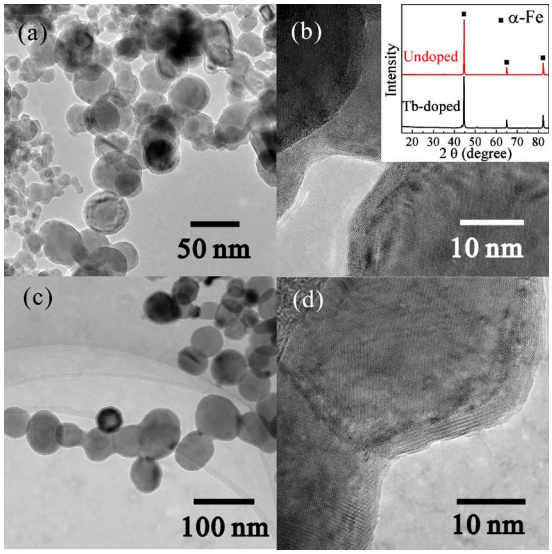

FIG. 1. (Color online) TEM images of the core-shell nanoparticles: (a) and (b) Tb-doped and (c) and (d) undoped Fe nanoparticles. The inset in (b) shows XRD patterns of the Tb-doped and undoped nanoparticles.

The shell oxides of the undoped Fe nanoparticles are, very likely, Fe_3O_4 or γ-Fe_2O_3,[4] that is, the undoped Fe nanoparticles are Fe/Fe-oxide nanocapsules. X-ray diffraction (XRD) data in the inset of Fig. 1(b) show that α-Fe peaks exist in both Tb-doped and undoped Fe nanoparticles, indicating that the main parts of the cores are Fe. Two or three weak peaks of γ-Fe (austenite) are visible for the Tb-doped Fe nanoparticles because of the use of carbon crucible. However, a small amount of Tb may exist in the core in the form of intermetallic compounds, such as $TbFe_2$ and Tb_2Fe_{17}, but very difficult to be detected. In order to investigate the surface compositions of the Tb-doped Fe nanoparticles, XPS spectra with etching times of 0 and 25 s were measured. It is anticipated that after the shell materials have been etched, new peaks of binding energies emerge if there are different valencies of some certain element in the core. The binding

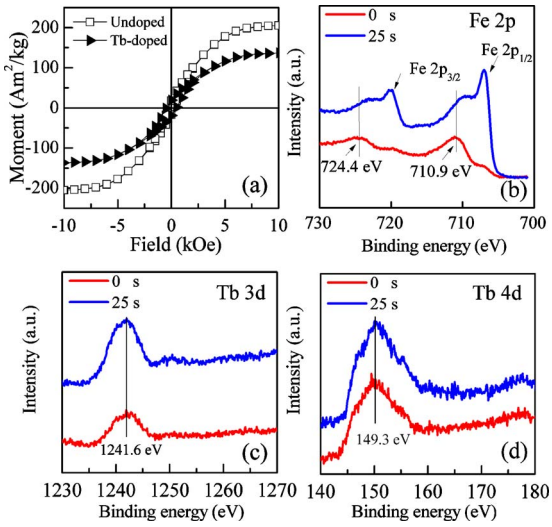

FIG. 2. (Color online) (a) Magnetic hysteresis loop at 295 K measured between 10 and −10 kOe of the Tb-doped and undoped nanoparticles. (b) Fe 2p, (c) Tb 3d, and (d) Tb 4d XPS spectra of the Tb-doped Fe nanoparticles.

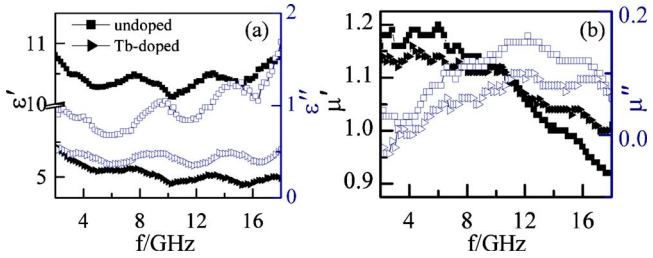

FIG. 3. (Color online) Frequency dependence of the complex permittivity and complex permeability of the Tb-doped and undoped Fe nanoparticles. Solid symbols represent the real parts of ε_r and μ_r, and the corresponding open ones represent the imaginary parts.

energies of Fe $2p_{3/2}$ and Fe $2p_{1/2}$ on the surface (etching time 0 s) of the Tb-doped Fe nanoparticles, as shown in Fig. 2(b), are 710.9 and 724.4 eV, respectively, which are in good agreement with the values reported for α-Fe_2O_3 and/or γ-Fe_2O_3.[10,11] When the etch time reached 25 s, the peaks of Fe ($2p_{3/2}$=707.1 eV and $2p_{1/2}$=720.3 eV) become dominant, indicating that the cores are less oxidized, or somehow "protected" by the surface oxidation.

Let us next discuss the effect of the terbium in the Tb-doped Fe nanoparticles. Figures 2(c) and 2(d) show the Tb 3d and 4d spectra. According to Fan *et al.*,[12] signals at 149.3 and 1241.6 eV are characteristic features of Tb^{3+}. The absence of signals around 156.9 and 164.5 eV excludes Tb^{4+} (Ref. 12), which is consistent with the well-established tripositive charge state in both Tb_2O_3 and Tb_2Fe_{17}. As no different binding energies of pure Tb were found with increasing etching time, Tb may present mainly in the Tb^{3+} oxidation state, probably Tb_2O_3, on the surface of the samples. Actually, in the formation process of nanocapsules during arc discharge, element with higher melting point will have the priority to condense, and the one with lower melting point will be richer in the shell.[13] The melting points of Tb and Fe are 1630 and 1809 K, respectively, which explains the rareness of Tb in the core part. As discussed above, the Tb-doped Fe nanoparticle can be defined as Fe-core/Fe_2O_3- and Tb_2O_3-shell nanocapsule.

Figure 3 shows the frequency dependencies of the EM parameters of the nanoparticles. After Tb doping, the complex permeability of nanoparticles remains almost unchanged, whereas the magnitude of the complex permittivity decreases substantially, from about $10.4-1.1j$ to about $5.1-0.5j$. This fluctuation behavior, with a few local maxima, can also be seen in the permittivity spectra. For metal-based nanocomposites, the space charge polarization and the dipole polarization mechanisms explain the absorption of energy by dielectrics, which influence the shape of the permittivity as a function of frequency. The significant fluctuations for ε' and ε'' have been found in carbon nanotubes that are ascribed to the displacement current lag at interfaces,[14] and in $Ni_{1-x}Co_xP$ alloy nanoparticles due to the ac loss.[15]

Figure 3(b) shows the frequency dependencies of the real (μ') and imaginary (μ'') parts of the permeability of the Tb-doped and/or undoped Fe nanoparticles. The μ' values of both the Tb-doped and undoped nanoparticles exhibit a general decrease with increasing frequency in the 2–18 GHz range. However, μ'' exhibits a broad maximum around about

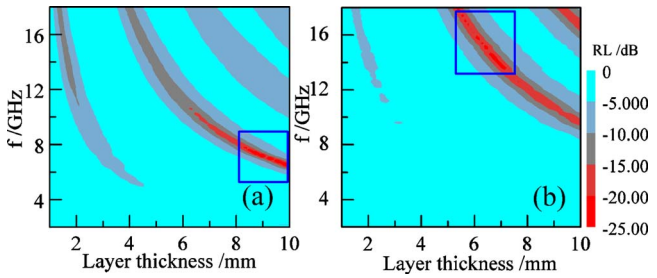

FIG. 4. (Color online) Color map of the RLs calculated from the measured EM-parameters of (a) undoped and (b) Tb-doped Fe nanoparticles.

10–13 GHz, with relative maxima at about 8, 12, and 17 GHz. The ferromagnetic resonance frequency f of soft-magnetic materials is often enhanced in nanoparticle because f increases with the magnetic anisotropy and small particles exhibit some surface anisotropy. The effect is enhanced by the Tb^{3+}, which has an aspherical 4f shell and therefore yields strong anisotropy contributions in noncubic atomic environments.[16] A similar mechanism also affects and generally enhances the damping.

Let us now discuss the usefulness of the present material for practical applications. RLs exceeding −20 dB mean 99% attenuation, which can be considered as an efficient absorption. Figure 4 shows the color maps of RL values calculated from the materials constants measured for the nanoparticles dispersed in paraffin, using Eq. (1). In both maps, ideal absorption (RL exceeding −20 dB) can be found, but in different ranges of d and f. The ideal absorption area (see the boxed areas in Fig. 4) of the Tb-doped Fe nanoparticles locates at thinner layer thicknesses and higher frequencies than that of undoped ones. One possible explanation for the improvement of the high-frequency absorption characteristics could be the crystal-field interaction of the Tb^{3+} ions.

Tinga *et al.* reported the permittivity and permeability of the multiphase inclusions in the form of confocal ellipsoidal shells dispersed in a host material,[17] which is very similar to the present core-shell system. According to his study, the absorption properties of the Fe-based nanoparticles-paraffin composites result from several factors, such as the material constants of shell and core materials, the size, the nanoparticles-to-paraffin mass ratios, and also the special core-shell structure with insulating oxide shells and ferromagnetic cores. The Tb doping changed both the microstructure and the composition of the Fe nanoparticles, which consequently changed the core-to-shell volume fraction, the boundary conditions of the Maxwell equations, the materials constants of the core-shell nanocomposites, and therefore the absorption properties.

IV. CONCLUSION

In summary, we have used arc discharge to synthesize Tb-doped and undoped Fe nanoparticles for microwave absorption and measured the permittivities and permeabilities of the Tb-doped and undoped particles in the frequency range of 2–18 GHz. With Tb doping, the microstructure and magnetic properties of Fe nanoparticles were changed, and thus the materials constants. Compared to the undoped particles, the maximum absorption of the Tb-doped Fe nanoparticles shifts to higher frequencies and thinner absorbing layer thicknesses. We tentatively ascribe this improvement to the anisotropy contribution of the Tb^{3+} ions, which affect both the resonance frequency and the line width.

ACKNOWLEDGMENTS

This work has been supported by the National Natural Science Foundation of China under Grant Nos. 50831006 and 50701045, and by the National Basic Research Program of China (Grant No. 2010CB934603), Ministry of Science and Technology China. Research at Nebraska was supported by NSF-MRSEC (Grant No. DMR-0820521) and NCMN.

[1] X. F. Zhang, X. L. Dong, H. Huang, Y. Y. Liu, W. N. Wang, X. G. Zhu, B. Lv, J. P. Lei, and C. G. Lee, Appl. Phys. Lett. **89**, 053115 (2006).
[2] X. G. Liu, D. Y. Geng, and Z. D. Zhang, Appl. Phys. Lett. **92**, 243110 (2008).
[3] Z. Han, D. Li, H. Wang, X. G. Liu, J. Li, D. Y. Geng, and Z. D. Zhang, Appl. Phys. Lett. **95**, 023114 (2009).
[4] B. Lu, X. L. Dong, H. Huang, X. F. Zhang, J. P. Lei, X. G. Zhu, and J. P. Sun, J. Magn. Magn. Mater. **320**, 1106 (2008).
[5] R. C. Che, L. M. Peng, X. F. Duan, Q. Chen, and X. Liang, Adv. Mater. **16**, 401 (2004).
[6] R. T. Lv, F. Y. Kang, J. L. Gu, X. C. Gui, J. Q. Wei, K. L. Wang, and D. H. Wu, Appl. Phys. Lett. **93**, 223105 (2008).
[7] P. Xu, X. J. Han, X. R. Liu, B. Zhang, C. Wang, and X. H. Wang, Mater. Chem. Phys. **114**, 556 (2009).
[8] E. Michielssen, J. M. Sajer, S. Ranjithan, and R. Mittra, IEEE Trans. Microwave Theory Tech. **41**, 1024 (1993).
[9] Y. W. Yun, S. W. Kim, G. Y. Kim, Y. B. Kim, Y. C. Yun, and Y. S. Lee, J. Electroceram. **17**, 467 (2006).
[10] J. L. Zhang, H. Ji, Y. G. Wei, Y. Wang, and N. Z. Wu, J. Phys. Chem. C **112**, 10688 (2008).
[11] J. D. Desai, H. M. Pathan, S. K. Min, K. D. Jung, and O. S. Joo, Appl. Surf. Sci. **252**, 1870 (2005).
[12] G. D. Fan, C. G. Feng, and Z. Zhang, J. Rare Earths **25**, 42 (2007) and references therein.
[13] D. Y. Geng, Z. D. Zhang, W. S. Zhang, P. Z. Si, X. G. Zhao, W. Liu, K. Y. Hu, Z. X. Jin, and X. P. Song, Scr. Mater. **48**, 593 (2003).
[14] P. C. P. Watts, D. R. Ponnampalam, W. K. Hsu, A. Barnes, and B. Chambers, Chem. Phys. Lett. **378**, 609 (2003).
[15] Y. J. Li, C. Z. Zhu, and C. M. Wang, J. Phys. D **41**, 125303 (2008).
[16] R. Skomski and J. M. D. Coey, *Permanent Magnetism* (Institute of Physics, Bristol, 1999).
[17] W. R. Tinga, W. A. G. Voss, and D. F. Blossey, J. Appl. Phys. **44**, 3897 (1973).